Estimation of Particle Flux Driven by Coherent Mode Using of Statistical Conditional Averaging

Yuichi KAWACHI, Sigeru INAGAKI[1,2], Kazunobu HASAMADA, Kotaro YAMASAKI[1], Fumiyoshi KIN, Yusuke KOSUGA[1,2], Makoto SASAKI[1,2], Yoshihiko NAGASHIMA[1,2], Naohiro KASUYA[1,2], Takuma YAMADA[1,3], Boyu ZHANG and Akihide FUJISAWA[1,2]

Interdisciplinary Graduate School of Engineering Sciences, Kyushu University, 6-1 Kasuga-koen, Kasuga 816-8580, Japan

[1] *Research Center for Plasma Turbulence, Kyushu University, 6-1 Kasuga-koen, Kasuga 816-8580, Japan*

[2] *Research Institution for Applied Mechanics, Kyushu University, 6-1 Kasuga-koen, Kasuga 816-8580, Japan*

[3] *Faculty of Arts and Science, Kyushu University, 744 Motooka, Nishi-ku, Fukuoka 819-0395, Japan*

(Received 30 January 2019 / Accepted 3 April 2019)

We proposed a new method to evaluate particle flux in magnetized turbulent plasma. To extract fundamental fluctuation pattern, we used template method which is a kind of statistical conditional averaging technique. The method allows as not only to extract coherent patterns of density and potential fluctuations but also to evaluate time delay between them. We succeeded to calculate particle flux driven by fluctuation pattern and observed this pattern drives inward particle flux. Result obtained by the method is in good agreement with that obtained by a conventional method.

Keywords: fluctuation, conditional average, particle flux

DOI: 10.1585/pfr.14.1402090

1. Introduction

At present anomalous transport observed in fusion devices is believed to be driven by turbulence [1]. In inhomogeneous magnetized plasma, fluctuations can be driven by several instability. However, there are few observations of turbulence driven transport.

Temporally and spatially simultaneous measurement of density and potential fluctuations allows us to estimate the particle flux. Potential fluctuation in low frequency (< ion cyclotron frequency) electrostatic turbulence can drive $B \times \nabla \tilde{\phi}$ drift (B is background magnetic field and $\tilde{\phi}$ is potential fluctuation) and the azimuthal electric field fluctuation and axial magnetic field drive radial motion of cylindrical plasma. Then the cross-phase between fluctuations of potential and density links to a time-averaged radial particle flux [2]. When the cross-phase is randomly changed over time, i.e. cross-coherence between fluctuations of potential and density is small, the time-averaged flux driven by such fluctuations is not significant. Although turbulence spectrum is usually broad, quasi-coherent fluctuations are thus important to evaluate particle flux experimentally.

Generally, it is difficult to simultaneously measure density and potential fluctuations at the same time and the same position. Furthermore, we should extract fluctuations synchronizing with one another. We have evaluated the temporal and spatial structure of quasi-coherent mode by statistical conditional average method so far [3]. If we apply conditional average to relatively coherent density and potential fluctuations in turbulent plasma, we can estimate particle flux driven by a structure in which density and potential fluctuations are synchronized. The purpose of this study is to develop an estimation method for particle flux driven by a fluctuating structure by conditional averaging.

2. Experimental Setup

Our experiment was performed in PANTA [4]. Experimental conditions are as follows; helicon wave input power of 6 kW, Argon gas pressure of 3 mTorr, and axial magnetic field of 1300 G. The plasma radius is about 50 mm. The typical electron density n_e and temperature T_e are $1.0 \times 10^{19}\,\mathrm{m}^{-3}$ and 3 eV, respectively. The turbulent fluctuations in PANTA are measured with electrostatic probe. Radial probe-array is installed at $z = 1375$ mm from helicon source of PANTA. The radial probe-array has 5 tips aligned at 1 cm radial intervals and is radially movable. In addition, azimuthal 64 channel probe-array is installed at $z = 1875$ mm from the helicon source as shown in Fig. 1. It can measure ion saturation current at $r = 4$ cm and 32 different azimuthal locations, simultaneously floating potential alternately in azimuthal direction. In PANTA, electron temperature fluctuation level is lower than density and potential fluctuations [5]. Thus, the ion saturation current fluctuation and the floating potential fluctuation can be considered as electron density fluctuation and space potential fluctuation respectively.

Typical time evolution and power spectrum density of ion saturation current observed in PANTA are shown in

---

author's e-mail: kawachi@riam.kyushu-u.ac.jp

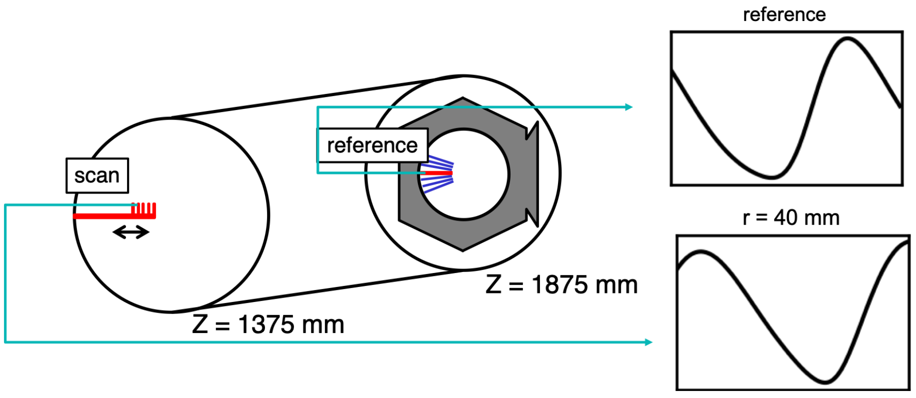

Fig. 1 Schematic view of probe set-up. Radial structure of potential and density fluctuations is reconstructed by conditional averaging with one of azimuthal probe as reference probe.

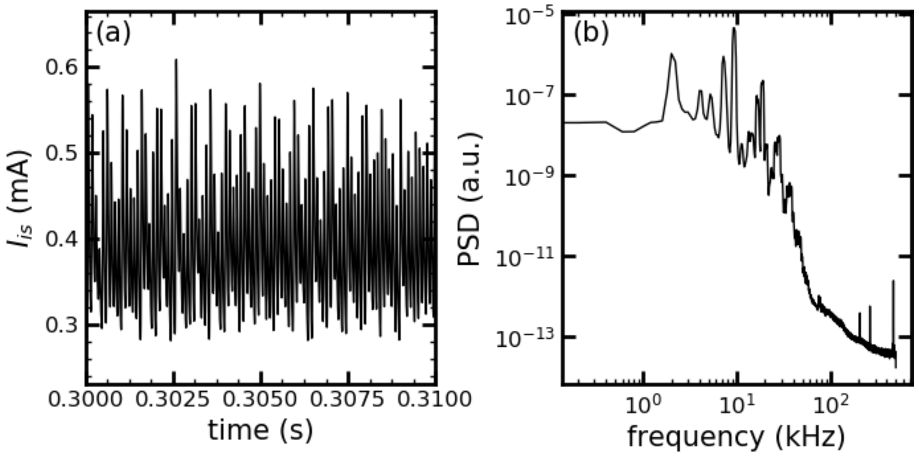

Fig. 2 (a) Typical time evolution of ion saturation current and (b) power spectrum density of ion saturation current.

Fig. 2. A coherent fluctuation with azimuthal mode number $m = 4$ and frequency $f \approx 9.2$ kHz is excited most strongly. Many fluctuations coexist in the ion saturation current signal. We home in on particle flux driven by a quasi-coherent structure related to this fluctuations.

3. Template Method

To reconstruct 2-dimensional structure of fluctuations, we applied conditional averaging technique to signals obtained with the azimuthal probe-array and radial probe-array. First, one of 64 ch probes was chosen as reference probe (Fig. 1). We tracked the timing of emergence of fluctuating pattern from the ion saturation current of the reference probe, then synchronized fluctuating patterns which are at 5 different radial locations are extracted based on the timing from the reference. Here, we used "Template method" [3, 6]. The radial probe measure not only ion saturation current but also floating potential in a shot-by-shot manner. Finally, we obtained temporal evolution of radial structure of fluctuating density and potential patterns.

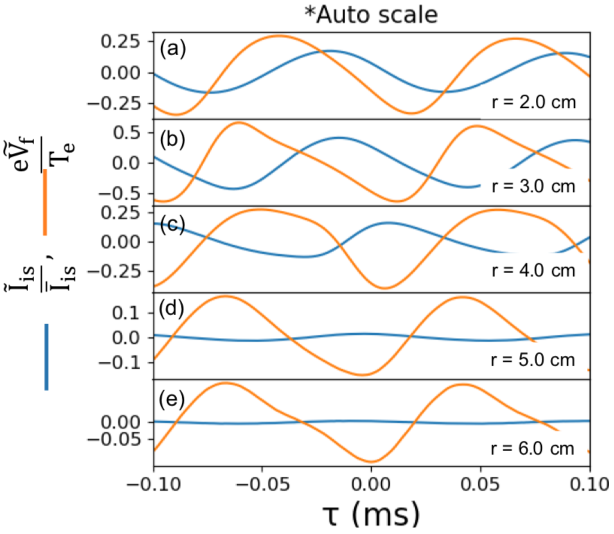

Fig. 3 (a-e) Conditional averaged wave forms of the coherent mode. Blue lines and orange lines are normalized ion saturation current and normalized potential, respectively.

The results of conditional averaging are shown in Fig. 3. We can see phase relation between the density and potential fluctuation of the coherent mode at each radial location. Fluctuation levels of density and potential is significantly different at $r > 5.0$ cm. In this region, the Boltzmann relationship is thus not satisfied.

4. Results

When phase difference between density and potential fluctuations exists, cross-field particle flux is driven through $E_\theta \times B$ flow $\tilde{v}_r$. The fluctuation-driven radial particle flux Γ_r is written as

$$\Gamma_r(t) = \tilde{n}(t)\tilde{v}_{E\times B,r}(t) = -\frac{\tilde{n}(t)\partial_\theta\tilde{\phi}(t)}{B}, \tag{1}$$

where $\tilde{n}$ and $\tilde{\phi}$ are density and potential fluctuation, respectively. Positive flux $\Gamma_r > 0$ means outward flux while negative flux $\Gamma_r < 0$ means inward flux. In order to calculate the particle flux, measurement of density and potential fluctuations at the same time and the same point is necessary. Our method can extract synchronized potential and density fluctuations at the same time and the same point.

In this study, we assumed that the fluctuation patterns rotates in the electron diamagnetic rotation as rigid-body and $m = 4$ structure. Azimuthal probe array supports this assumption at $r = 4$ cm. We can transform the time to the azimuthal location. Then, the differential operator can be replaced ∂_θ to ∂_t as follow

$$\Gamma_r(t) = -\frac{\langle\tilde{n}(t)\rangle}{B}\left\langle\frac{\partial\tilde{\phi}(t)}{\partial t}\Big/\frac{\partial\theta}{\partial t}\right\rangle = \frac{k_\theta}{2\pi f}\frac{\langle\tilde{n}(t)\rangle\left\langle\partial_t\tilde{\phi}(t)\right\rangle}{B}, \tag{2}$$

where ⟨⟩ means conditional averaging.

In this way, we estimated temporal evolution of particle flux driven by the pattern and it is as shown in Figs. 4 (a-e). The particle flux was localized around $r = 3.0$ cm and the direction of time-averaged particle flux is inward. Radial profile of the time averaged particle flux was also evaluated as shown in Fig. 5. Inward particle flux was observed in the regime of $r = 2.0$ - 3.0 cm. Similar results of inward flux driven by parallel velocity shear driven mode in PANTA [4] and electron temperature driven mode in LVPD [7] are also observed.

Nonlinear wave coupling is observed by bicoherence analysis at $r = 4.3$ cm where waveform is strongly distorted and higher harmonics of the fundamental mode become large [3]. While particle flux driven by the higher harmonics is small at the position, particle flux driven by the fundamental mode becomes large through increase in the cross-phase. This suggests that nonlinear process modulating the fundamental mode relates to increase in the cross-phase of the fundamental mode.

Level of potential fluctuation of the quasi-coherent structure is larger than level of the density fluctuation, and this structure drives inward particle transport. Thus, this structure is considered to not be drift wave. In future work, to identify this mode we will measure parallel and azimuthal flows and temperature fluctuation.

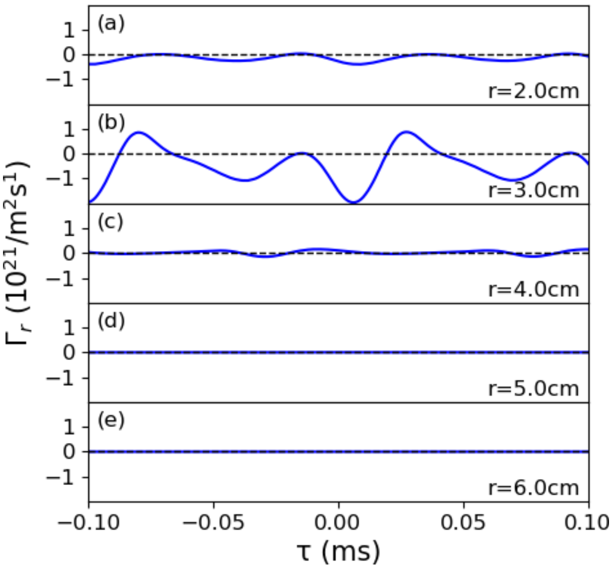

Fig. 4 (a-e) Estimated time evolution of particle flux driven by the coherent pattern. Negative flux means radial inward flux, and vice versa.

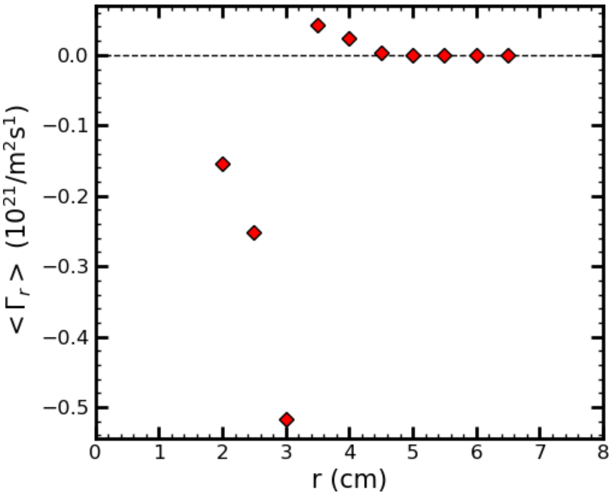

Fig. 5 (a) Radial profile of averaged particle flux of the coherent pattern.

5. Discussion

We assumed that density fluctuations which have weak auto-correlation have weak cross-correlation with potential fluctuations. If density fluctuations which have weak auto-correlation but significant cross-correlation with potential fluctuations are excited, finite instantaneous flux is driven by such fluctuations and the flux will not be canceled out after conditional averaging.

To check this, we have calculated an instantaneous flux ($\left\langle\tilde{n}\partial_\theta\tilde{\phi}\right\rangle/B$) by using 4-tips probe which is located at $z = 1125$ mm from plasma source. It is radially movable, and two probe tips can measure ion saturation current and others can measure floating potential [4]. The interval be-

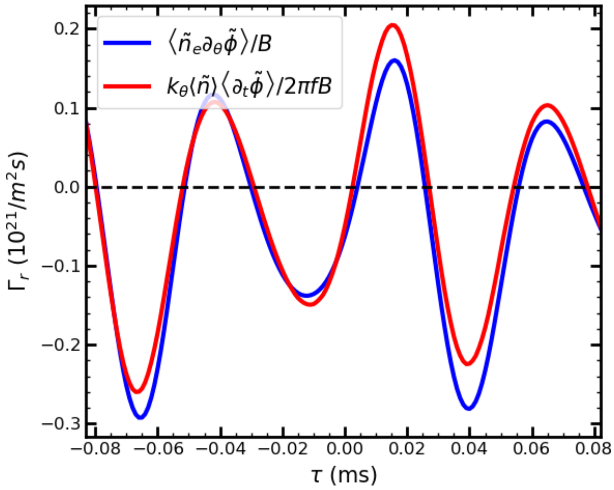

Fig. 6 Time evolution of particle flux measured by 4-tips probe. Blue line is particle flux evaluated by conditional averaged potential and density. Red line is particle flux evaluated by conditional averaged instantaneous particle flux.

tween the tips is about 5.5 mm ($< \lambda_\theta \approx 60$ mm), then we can measure density and potential at the same time and the same point. Thus, it can evaluate flux directly. We applied conditional averaging based on the trigger function obtained from density fluctuation to the instantaneous flux, and compared it with that evaluated by our method ($k_\theta \langle n \rangle \langle \partial_t \phi \rangle / 2\pi f B$). Figure 6 demonstrates that the two are almost the same.

To compare with conventional method, we also applied cross spectrum analysis [8]. Radial particle flux in frequency domain is written as,

$$\langle \Gamma_r(f') \rangle_{\mathrm{ave}} = \frac{2}{B} k_\theta \int_{f'-\Delta f/2}^{f'+\Delta f/2} \gamma_{\tilde{n},\tilde{\phi}}(f) |P_{\tilde{n}}(f)|^{1/2} |P_{\tilde{\phi}}(f)|^{1/2} \sin(\alpha_{\tilde{n},\tilde{\phi}}(f)) df, \tag{3}$$

where $\langle\rangle_{\mathrm{ave}}$ means long time averaging, f' and Δf are frequency of fluctuations and frequency resolution, respectively. $\gamma_{\tilde{n},\tilde{\phi}}$ and $\alpha_{\tilde{n},\tilde{\phi}}$ are cross-coherence and cross-phase calculated by cross spectrum between density and potential fluctuations. $P_{\tilde{n}}$ and $P_{\tilde{\phi}}$ are power spectrum of density and potential fluctuations, respectively. Azimuthal wave number, $k_\theta = m/r$ is $100\,\mathrm{m}^{-1}$ and frequency is 9.2 kHz in this study. Our method is also applied to 4 tips probe signals with one of the azimuthal probe array as a reference probe.

Results of three methods (our method, conditional averaging of the instantaneous flux and conventional spectrum method) are compared in Fig. 7. We observed inward particle flux in three methods. Particle flux estimated by our method is greater than that estimated from single frequency component. On the other hands, particle flux estimated from all frequency components is greater than from our method. This result is consistent because our method extracts not only the fundamental frequency component but also higher harmonics. Many quasi-coherent structures usually co-exist in plasma turbulence. In this case, we have to find all quasi-coherent structures to evaluate total flux. Our method can evaluate flux driven by quasi-coherent pattern of interest.

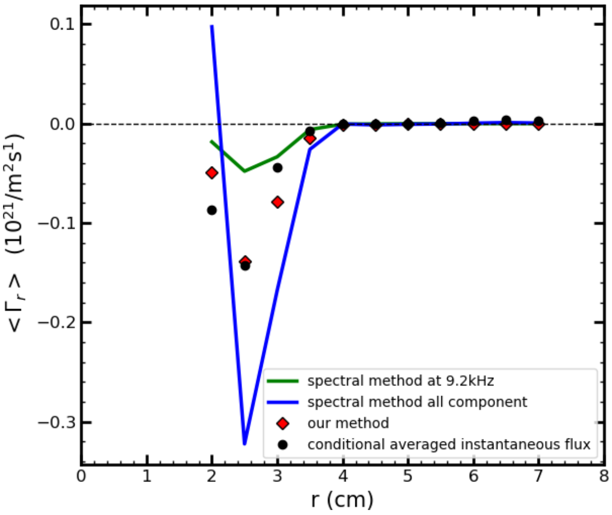

Fig. 7 (a) Comparison of radial profiles of averaged particle flux. Green line and blue line indicate particle flux estimated by spectral analysis. Green line consists of only the fundamental frequency component of the coherent mode. Blue line consists of all frequency components. Black dots are conditional averaged instantaneous flux and red diamonds indicate particle flux estimated by our method. Our method include the fundamental frequency components of the coherent mode and its synchronizing components (e.g. higher harmonics).

6. Summary

In summary, statistical averaging analysis was applied to the quasi-coherent mode observed in PANTA, to extract its spatiotemporal structure and particle flux. This analysis revealed the features of quasi-coherent mode such as (i) spatiotemporal structure of density and potential structure, (ii) fluctuation driven inward particle flux. Verification of our method was performed and its results indicated our method can estimate particle flux driven by synchronous density and potential fluctuations.

Acknowledgments

This work was partially supported by the Grant-in-Aid for Scientific Research of JSPS of Japan (JP18K03578, JP17H06089, JP17K06994, JP15H02155, JP15H02335), the collaborative Research Program of Research Institute for Applied Mechanics, Kyushu University and of NIFS (NIFS13KOCT001).

[1] A.J. Wootton *et al.*, Phys. Fluids B **2**, 2879 (1990).
[2] W. Horton, Rev. Mod. Phys. **71**, 735 (1999).

[3] Y. Kawachi *et al.*, Plasma Fusion Res. **13**, 3402102 (2018).
[4] S. Inagaki *et al.*, Sci. Rep. **6**, 22189 (2016).
[5] K. Kawashima *et al.*, Plasma Fusion Res. **6**, 2406118 (2011).
[6] S. Inagaki *et al.*, Plasma Fusion Res. **9**, 1201016 (2014).
[7] P. Srivastava *et al.*, Phys. Plasmas **6**, 22189 (2017).
[8] F. Kin *et al.*, J. Phys. Soc. Jpn. **85**, 093501 (2016).